Nanoscale

RSC Publishing

COMMUNICATION

View Article Online
View Journal | View Issue

Cite this: *Nanoscale*, 2013, **5**, 3643

Received 15th December 2012
Accepted 15th March 2013

DOI: 10.1039/c3nr34123b

www.rsc.org/nanoscale

Mechanically resilient electrospun TiC nanofibrous mats surface-decorated with Pt nanoparticles for oxygen reduction reaction with enhanced electrocatalytic activities†

Hai-jing Liu,[a] Feng Wang,*[a] Yong Zhao[b] and Hao Fong*[b]

Mechanically resilient mats consisting of overlaid electrospun nanofibers with self-generated TiC crystallites embedded in a carbon matrix are surface-decorated with Pt nanoparticles as a novel electrocatalytic system for oxygen reduction reaction. Electrocatalytic activities (*e.g.*, on-set potential and current density) of Pt are substantially enhanced due to high specific surface area of the support and the synergetic effect of TiC and Pt on electrocatalysis.

Oxygen reduction reaction (ORR) is one of the most important electrochemical reactions in energy-conversion devices (*e.g.*, fuel cells[1,2] and metal–air batteries[3,4]). Nonetheless, the sluggish kinetics of ORR resulting from high over-potentials (*i.e.*, up to 300 mV)[5,6] limits these devices from practical applications[7,8] even with Pt nanoparticles (NPs) supported on carbonaceous materials, which are considered as the best electrocatalytic system for ORR.[9] Hence, numerous research efforts have been devoted to optimize the electrocatalytic systems to improve the kinetics of ORR, for example, alloying Pt with transition metals such as Fe, Co, or Ni[10,11] and/or developing alternative support materials.[12,13] Carbonaceous materials (*e.g.*, carbon black Vulcan XC-72) have been widely adopted as the support for fabrication of commercial electrocatalytic systems with Pt NPs, despite several problems (including the inconvenient pre-treatment procedure and the instability under certain operational conditions) still existing.[14,15]

Recently, the electrocatalytic systems based on Pt NPs supported on non-carbonaceous materials such as WC,[16] WO_3,[17] and TiO_2 (ref. 18) have been studied by several research groups. Their results indicated that the electrocatalytic activities of Pt could be significantly improved due to strong interactions between Pt NPs and their supporting materials. Albeit these non-carbonaceous materials appear promising for making highly efficient electrocatalytic systems of ORR, some obstacle issues (*e.g.*, small specific surface area and low stability) are still under further investigations.[16] Herein mechanically resilient mats, consisting of overlaid nanofibers with self-generated TiC crystallites (~70 wt%) embedded in the matrix of carbon (~30 wt%), have been prepared *via* the nanomaterial-processing technique of electrospinning[19–21] followed by the treatment of carbothermal reduction.[22] The prepared electrospun TiC nanofibrous mats have been studied as the novel support for Pt NPs. Compared with other supporting materials, the TiC mats possess the following advantageous characteristics/properties: (1) TiC has high melting point, hardness, and wear resistance, thus it is stable in practical applications; (2) the specific surface area of TiC mats is ~500 $m^2 g^{-1}$, which is much larger than that of Vulcan XC-72 or the reported non-carbonaceous support materials, thus the agglomeration of Pt NPs would be mitigated; (3) the TiC nanofibrous mats are mechanically resilient and can be readily assembled into electrodes without bonding agents.

To the best of our knowledge, few investigations have been carried out on electrocatalytic behaviors of TiC or TiC supported catalysts for ORR. In this research, the electrocatalytic systems of Pt NPs supported on commercial carbon paper (BO030, used for fuel cells, Toray, Japan), electrospun polyacrylonitrile-based carbon nanofibrous mat (ECNF mat, prepared *via* the method reported previously[23]), and electrospun TiC nanofibrous mat were studied, and the results indicated that the novel system of the TiC mat surface-decorated with Pt NPs demonstrated the highest electrocatalytic activities for ORR under both acidic and alkaline conditions. Additionally, the TiC mat without Pt NPs also exhibited catalytic activity for ORR in alkaline solutions, suggesting that it might be promising for the development of Pt-free electrocatalytic systems.

As shown in the inset of Fig. 1a, the overlaid mat of continuous electrospun TiC nanofibers was mechanically resilient. A

[a]*State Key Laboratory of Chemical Resource Engineering, Beijing Key Laboratory of Electrochemical Process and Technology for Materials Beijing University of Chemical Technology, 15 Bei-San-Huan East Road, Beijing 100029, P. R. China. E-mail: wangf@mail.buct.edu.cn; Fax: +86 10 64451996; Tel: +86 10 64451996*

[b]*Department of Chemistry and Applied Biological Sciences, South Dakota School of Mines and Technology, 501 East Saint Joseph Street, Rapid City, SD 57701, USA. E-mail: hao.fong@sdsmt.edu; Fax: +1 605 394 1229; Tel: +1 605 394 1232*

† Electronic supplementary information (ESI) available. See DOI: 10.1039/c3nr34123b

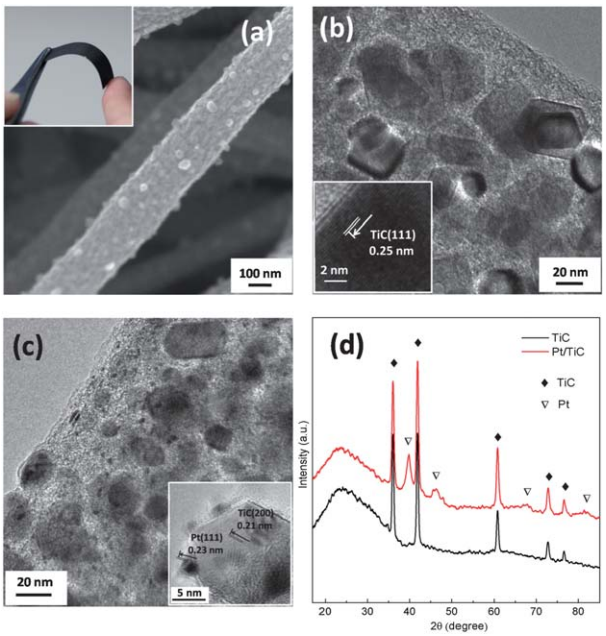

Fig. 1 (a) SEM image of a representative nanofiber in the electrospun TiC nanofibrous mat (with the inset showing a photograph of the mat). (b) TEM image of the TiC nanofiber prior to surface decoration with Pt NPs. (c) TEM image of the TiC nanofiber after surface decoration with Pt NPs. (d) XRD patterns of electrospun TiC nanofibrous mats before and after the surface-decoration with Pt NPs.

typical scanning electron microscopy (SEM) image (Fig. 1a) indicated that the nanofibers had diameters of ~180 nm with particles having sizes of tens of nanometers on their surface. A typical transmission electron microscopy (TEM) image (Fig. 1b) of the nanofibers revealed that a large amount of particles with sizes in the range of 5–30 nm were randomly distributed in the matrix of carbon. As evidenced from the high-magnification TEM image (the inset in Fig. 1b), the particles were crystalline and the interplanar spacing (*i.e.*, *d*-spacing) was 0.25 nm, which was consistent with the (111) plane of TiC crystallites according to JCPDS 65-8808. The X-ray diffraction (XRD) patterns of the TiC nanofibrous mat in Fig. 1d (black line) exhibited five diffraction peaks centered at 36°, 42°, 61°, 72°, and 76°, which could be assigned to the crystallographic planes of (111), (200), (220), (311), and (222) for TiC crystallites with cubic structures, respectively.

As shown in Fig. 1c and S1 (in the ESI†), Pt NPs with very small particle sizes of a few nanometers were randomly decorated on the surface of TiC nanofibers. Most of the Pt NPs were distributed on TiC crystallites, while some were located on the matrix of carbon. The *d*-spacings of Pt NPs and TiC crystallites were measured as 0.23 nm and 0.21 nm, respectively; these were consistent with the reported values of the (111) plane of cubic Pt and (200) plane of cubic TiC. The XRD patterns of the Pt/TiC system further confirmed the presence of both TiC crystallites (JCPDS 65-8808) and Pt NPs (with fcc structures, JCPDS 65-2868). Compared with the Pt NPs supported on commercial carbon paper, ECNF mat, and the reported non-carbonaceous supporting materials,[16–18] the Pt NPs on the electrospun TiC nanofibrous mat were smaller. This was attributed to different specific surface areas of supporting materials: the specific surface area of the electrospun TiC nanofibrous mat was measured at 499.5 $m^2 g^{-1}$ according to the Brunauer–Emmett–Teller (BET) nitrogen adsorption–desorption method, while the BET surface areas of carbon paper, ECNF mat, and the reported WC support were 0.83 $m^2 g^{-1}$, 19.1 $m^2 g^{-1}$, and 143 $m^2 g^{-1}$, respectively. The high specific surface area of the TiC mat resulted in uniform dispersion and small sizes of Pt NPs, further leading to the enhancement of electrocatalytic activities.

Electrocatalytic properties of the TiC nanofibrous mat surface-decorated with Pt NPs were evaluated, and the results were compared to those acquired from the carbon paper and ECNF mat both surface-decorated with Pt NPs as well. The deposition of Pt NPs on the three supports was conducted by the same procedure with Pt loading amounts of approximately the same at 7.5 wt %. Electrocatalytic properties of the TiC nanofibrous mat without Pt NPs were also studied as a blank/control sample. The current densities in the plotted cycle voltammetry (CV) and polarization curves were normalized to the geometric surface area of the electrode. Initially, the CV measurements were carried out in the range from −0.3 to 1.0 V (*vs.* SCE) in 0.5 M H_2SO_4 solution at a scan rate of 50 mV s^{-1} (Fig. S2 in the ESI†). The electrochemically active surface area (ECSA) of each catalyst was calculated *via* integrating the area under the peak of hydrogen desorption.[24] Based on the fact that the charge required to oxidize one monolayer of hydrogen on Pt was 0.21 (mC cm^{-2}),[25] the Pt/TiC system had the calculated ECSA value of 100.5 $m^2 g^{-1}$, which was much larger than the systems of Pt/carbon paper (47.6 $m^2 g^{-1}$) and Pt/ECNF (63.0 $m^2 g^{-1}$). The high value of ECSA for the Pt/TiC system was primarily due to the extremely small particle sizes and uniform/random dispersion of Pt NPs.

The electrocatalytic behaviors for ORR were studied under both acidic (0.1 M $HClO_4$ solution) and alkaline (1.0 M NaOH solution) conditions, and CV curves of the four electrocatalytic systems in O_2 saturated solutions are shown in Fig. 2a and b. In

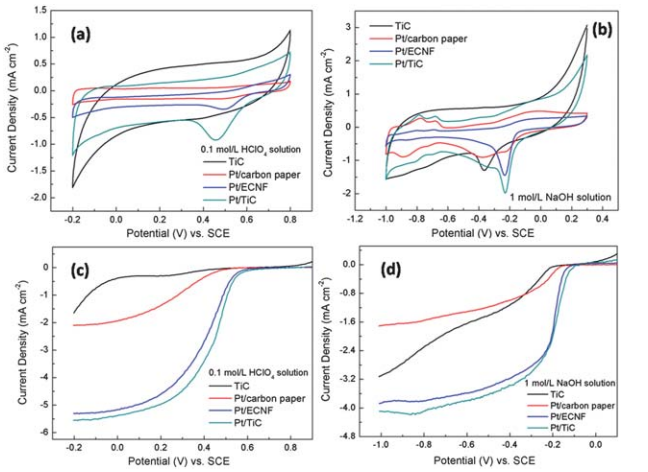

Fig. 2 CV curves obtained from the 4 electrocatalytic systems of TiC, Pt/carbon paper, Pt/ECNF, and Pt/TiC in (a) 0.1 M $HClO_4$ and (b) 1.0 M NaOH solutions scanned at 50 mV s^{-1} with a rotating rate of 1600 rpm, and polarization curves showing the ORR current densities for the 4 systems in (c) 0.1 M $HClO_4$ and (d) 1.0 M NaOH solutions scanned at 5 mV s^{-1}.

the acidic solution, the Pt/TiC system exhibited the largest reduction current density for ORR in the potential range from 0.3 to 0.6 V (*vs.* SCE), while TiC did not show any catalytic activities. In the alkaline solution, CV curves for the Pt/TiC system also exhibited the largest reduction current density for ORR compared with the systems of Pt/carbon paper and Pt/ECNF. Additionally, the electrospun TiC nanofibrous mat without Pt NPs also showed the electrocatalytic activity. Although such an activity occurred at a more negative potential, the reduction current density was larger than that of the Pt/carbon paper system while similar to that of the Pt/ECNF system.

The polarization curves in Fig. 2c and d depict ORR currents for the four systems of TiC, Pt/carbon paper, Pt/ECNF, and Pt/TiC in both acidic and alkaline solutions. The technique of rotating disk electrode (RDE) at 1600 rpm was adopted in this study. The polarization curves indicated that the ORR occurred under mixed kinetic-diffusion control at a high potential region followed by a plateau of diffusion limiting current, which would depend upon the rotating rate. The on-set and half-wave potentials, as well as diffusion-limit current densities are summarized in Tables S1 and S2 (in the ESI†). It was evident that the on-set potential of the Pt/TiC system was shifted to more positive values as compared to those of Pt/ECNF and Pt/carbon paper systems in the acidic solution (Fig. 2c). At the half-wave potentials, the ORR current density generated by the Pt/TiC system was 1.6 times larger than that of the Pt/carbon paper system. In the alkaline solution, similar results were observed; moreover, the TiC mat without Pt NPs was also electrocatalytically active, exhibiting even larger current density for ORR than the system of Pt/carbon paper at the potentials lower than −0.33 V (*vs.* SCE).

The ORR kinetics of TiC, Pt/carbon paper, Pt/ECNF, and Pt/TiC systems were further investigated *via* the calculation of electron transfer numbers by the Koutecky–Levich equation[26,27] (Fig. S3, Tables S1 and S2 in the ESI†) and mass-transport corrected Tafel slopes normalized to the ECSA of electrocatalysts (Fig. 3a and b). As summarized in Table S1,† O_2 was mainly reduced through a four-electron pathway with the electrocatalytic systems of Pt/TiC and Pt/ECNF in both acidic and alkaline solutions, while the Pt/carbon paper system mainly resulted in a two-electron ORR process due to low coverage of Pt NPs on carbon paper, where the ORR could be catalyzed by carbon paper *via* the two-electron pathway.[28] Unlike other non-metal electrocatalysts (*e.g.*, MnO_2 (ref. 29)), the number of electrons transferred per O_2 molecule for the TiC nanofibrous mat without Pt NPs was 3.8, suggesting a predominantly four-electron pathway for ORR.

The kinetics regarding the adsorption mechanism of O_2 was evaluated from Tafel slopes. The diffusion-current-corrected Tafel slopes of the four electrocatalytic systems under acidic and alkaline conditions are shown in Fig. 3a and b, respectively. The results indicated that the Pt/TiC system maintained the highest kinetic currents over the Tafel range compared to the systems of Pt/carbon paper and Pt/ECNF under both acidic and alkaline conditions. In 0.1 M $HClO_4$ solution, the Tafel plots exhibited two different slopes at low and high over-potential

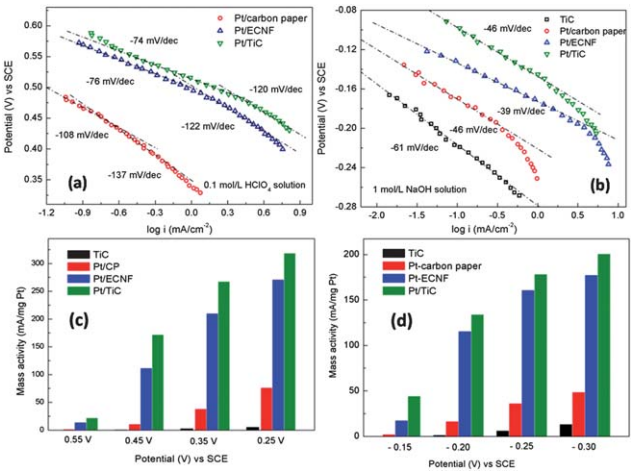

Fig. 3 Tafel slopes of the 3 electrocatalytic systems of Pt/carbon paper, Pt/ECNF and Pt/TiC in (a) 0.1 M $HClO_4$ and (b) 1.0 M NaOH solutions. Mass activities of the 4 systems at different potentials in (c) 0.1 M $HClO_4$ and (d) 1.0 M NaOH solutions.

ranges. The Tafel slopes of −60 and −120 mV dec^{-1} were typically reported in the absence of Nafion in the catalyst layer and with a low loading amount of Pt, assuming 100% catalyst utilization.[30] The obtained Tafel slopes for the Pt/TiC system (−74 and −120 mV dec^{-1}) were close to the reported values while smaller than those for the systems of Pt/ECNF and Pt/carbon paper, indicating the high utilization of Pt on TiC and a possible improvement in the kinetics of ORR by utilizing Pt on TiC rather than on carbon. In 1.0 M NaOH solution, only the Tafel slopes in the range of low current density needs to be calculated.[31] The acquired results were similar to the reported values in alkaline solutions.[31] As shown in Fig. 3b, the Tafel slope for Pt/TiC in alkaline solution was larger than that for Pt/ECNF. This might be due to the fact that the high surface area of the TiC nanofibrous mat would result in strong chemisorption of oxygen-generated species (*e.g.*, OH_{ad}) during the ORR process in concentrated solutions.[32]

Calculated from polarization curves obtained at 1600 rpm, the corresponding ORR mass activities of the four electrocatalytic systems under acidic and alkaline conditions are shown in Fig. 3c and d, respectively. The current densities were converted to the mass activities of Pt on different supports. The data acquired from the TiC mat without Pt are also shown for comparison. In both acidic and alkaline solutions, the Pt/TiC system had the highest mass activities at various potentials. The mass activity of the Pt/ECNF system was smaller than that of the Pt/TiC system, but it was still several times larger than that of the Pt/carbon paper system. Note that the TiC mat without Pt also exhibited activities for ORR in alkaline solution in a high over-potential range.

Despite that the TiC mat without Pt did not show the electrocatalytic activity for ORR under acidic conditions, the attachment of Pt NPs on TiC crystallites significantly improved the ORR performance as compared to the attachments of Pt NPs on ECNF and carbon paper. The high surface area of the electrospun TiC nanofibrous mat (*i.e.*, the support) not only facilitated the uniform/random dispersion of Pt nanoparticles on the

surface, but also enhanced the mass charge transport by providing an increased effective length and an improved electrode–electrolyte contact area, similar to the enhancement of carbonaceous support materials.[33,34] Although it might be premature to propose a mechanism, according to experimental results and the published research on WC,[16] it is evident that there is a synergetic effect of TiC and Pt through the electron transfer, which is quite different from that of Pt and carbonaceous materials[35–37] due to the different crystalline and morphological structures. Under alkaline conditions, the TiC crystallites in nanofibers promoted the catalytic activity of Pt as well; additionally, they also exhibited the catalytic activity for ORR mainly through a four-electron pathway, which had not been discovered in other non-metal electrocatalytic materials. Albeit the catalytic performance of TiC alone was not as high as that of Pt, the cost-effectiveness and the electrochemical resistance made it promising as an alternative to noble metal catalysts.

Conclusions

In summary, the electrospun TiC nanofibrous mat surface-decorated with Pt NPs was explored as a novel electrocatalytic system for ORR under both acidic and alkaline conditions. Compared with commercial carbon paper and the ECNF mat, the TiC mat had much larger specific surface area; hence, Pt NPs could be uniformly/randomly dispersed on the fiber surface with smaller particle sizes, leading to the higher degree of utilization of Pt and substantially enhanced electrocatalytic activities. The Pt/TiC system exhibited higher electrocatalytic activities for ORR in terms of on-set potential, kinetic current and mass activity than the systems of Pt/ECNF and Pt/carbon paper. Additionally, the TiC nanofibrous mat without Pt NPs was also active for ORR under alkaline conditions, indicating that the TiC mat alone could be utilized as a low-cost alternative for Pt-based electrocatalysts.

Experimental

Preparation

Electrospun TiC nanofibrous mats[22] and electrospun polyacrylonitrile-based carbon nanofibrous (ECNF) mats[23] were prepared by following the procedures reported previously. For the attachment of Pt NPs, a TiC mat (0.05 g) was immersed in 10 mL of 0.002 M H_2PtCl_6 solution for 24 h; subsequently, 10 mL of 0.02 M $NaBH_4$ solution was added drop-wise. The mixture was then kept for 3 h to complete the reduction of the Pt precursor. The acquired mat was rinsed with distilled water several times before being dried at 60 °C under vacuum. The ECNF mat and carbon paper surface-attached with Pt NPs were prepared *via* the same procedure.

Characterization

Morphologies and structures of the prepared samples were examined with a field emission SEM (FE-JSM-6701F, JEOL) and a TEM (JSM-2100, JEOL). XRD studies were carried out on a Rigaku D/max-2500 XRD with Cu Kα (λ = 1.54 Å). Specific surface areas were measured by the BET nitrogen adsorption–desorption method using the equipment of Quantachrome AUTOSORB-1.

Electrochemical measurements

For the preparation of testing electrodes, each electrocatalytic system (5 mg) was first mixed with 0.05 mL of Nafion (5.0 wt%) and 1.0 mL of ethanol followed by ultrasonication for 2 h. A measured volume (0.009 mL) was then transferred *via* a syringe onto a freshly polished glassy carbon electrode (0.071 cm^2 for CV measurements and 0.2472 cm^2 for RDE), and the solvent was evaporated at room temperature. Thereafter, electrochemical measurements were carried out using the M273A Potentiostat/Galvanostat (Princeton Applied Research, USA) and a conventional three-electrode cell. The counter electrode was Pt foil, and a saturated calomel electrode (SCE) was used as the reference electrode. The catalytic activity for ORR was measured with an apparatus of rotating disk electrode (RDE) (Princeton Applied Research, USA). High-purity nitrogen/oxygen was used for deaeration. During the measurements, a constant flow of nitrogen/oxygen was kept above the electrolyte surface. All electrochemical experiments were performed in a thermostatted cell at 30 °C.

Acknowledgements

This research was supported by the (Chinese) National Science Fund for Distinguished Young Scholars (Award number: 51125007) and by the (U.S.) Department of Energy (Award number: DE-FG02-08ER64624).

Notes and references

1 A. J. Appleby, *J. Electroanal. Chem.*, 1993, **357**, 117–179.
2 E. Yeager, *Electrochim. Acta*, 1984, **29**, 1527–1537.
3 Y. Lu, Z. Xu, H. A. Gasteiger, S. Chen, K. Hamad-Schifferli and Y. Shao-Horn, *J. Am. Chem. Soc.*, 2010, **132**, 12170–12171.
4 Z. Chen, A. Yu, D. Higgins, H. Li, H. Wang and Z. Chen, *Nano Lett.*, 2012, **12**, 1946–1952.
5 S. Arico, S. Srinivasan and V. Antonucci, *Fuel Cells*, 2001, **1**, 133–161.
6 H. A. Gasteiger, S. S. Kocha, B. Sompalli and F. T. Wagner, *Appl. Catal., B*, 2005, **56**, 9–35.
7 J. K. Nørskov, J. Rossmeisl, A. Logadottir, L. Lindqvist, J. R. Kitchin, T. Bligaard and H. Jonsson, *J. Phys. Chem. B*, 2004, **108**, 17886–17892.
8 R. R. Adzic, in *Electrocatalysis*, ed. J. Lipkowski and P. N. Ross, Wiley, New York, 1998, p. 197.
9 K. Kinoshita, in *Electrochemical Oxygen Technology*, J. Weiley and Sons, New York, 1992.
10 V. R. Stamenkovic, B. S. Mun, M. Arenz, K. J. J. Mayrhofer, C. A. Lucas, G. Wang, P. N. Ross and N. M. Markovic, *Nat. Mater.*, 2007, **6**, 241–247.
11 T. Toda, H. Igarashi, H. Uchida and M. Watanabe, *J. Electrochem. Soc.*, 1999, **146**, 3750–3756.
12 S. H. Tang, G. Q. Sun, J. Qi, S. G. Sun, J. S. Guo and Q. Xin, *Chin. J. Catal.*, 2010, **31**, 12–17.

13 Z. Wen, J. Liu and J. Li, *Adv. Mater.*, 2008, **20**, 743–747.
14 W. M. Chen, Q. Xin, G. Q. Sun, Q. Wang, Q. Mao and H. D. Su, *J. Power Sources*, 2008, **180**, 199–204.
15 J. Suntivich, K. J. May, H. A. Gasteiger, J. B. Goodenough and Y. Shao-Horn, *Science*, 2011, **334**, 1383–1385.
16 Y. Liu and W. E. Mustain, *ACS Catal.*, 2011, **1**, 212–220.
17 Y. Liu, S. Shrestha and W. E. Mustain, *ACS Catal.*, 2012, **2**, 456–463.
18 S. Huang, P. Ganesan and B. N. Popov, *ACS Catal.*, 2012, **2**, 825–831.
19 D. H. Reneker and I. Chun, *Nanotechnology*, 1996, **7**, 216–223.
20 Z. Huang, Y. Zhang, M. Kotaki and S. Ramakrishna, *Compos. Sci. Technol.*, 2003, **63**, 2223–2253.
21 A. Greiner and J. H. Wendorff, *Angew. Chem., Int. Ed.*, 2007, **46**, 5670–5703.
22 L. Zhang, J. Hu, A. A. Voevodin and H. Fong, *Nanoscale*, 2010, **2**, 1670–1673.
23 J. Liu, Z. Yue and H. Fong, *Small*, 2009, **5**, 536–542.
24 Q. Huang, H. Yang, T. Tang, T. Lu and D. L. Akins, *Electrochem. Commun.*, 2006, **8**, 1220–1224.
25 L. Bal, L. Gao and B. E. Conway, *J. Chem. Soc., Faraday Trans.*, 1993, **89**, 235–242.
26 H. M. Villullas and M. Lopez Teijelo, *J. Electroanal. Chem.*, 1995, **385**, 39–44.
27 S. Kondo, M. Nakamura, N. Maki and N. Hoshi, *J. Phys. Chem. C*, 2009, **113**, 12625–12628.
28 J. Guo, A. Hsu, D. Chu and R. Chen, *J. Phys. Chem. C*, 2010, **114**, 4324–4330.
29 I. Roche and K. Scott, *J. Electroanal. Chem.*, 2010, **638**, 280–286.
30 Y. E. Seidel, A. Schneider, Z. Jusys, B. Wickman, B. Kasemo and R. J. Behm, *Faraday Discuss.*, 2009, **140**, 167–184.
31 I. Roche, E. Chaînet, M. Chatenet and J. Vondrák, *J. Phys. Chem. C*, 2007, **111**, 1434–1443.
32 V. Komanicky, A. Menzel and H. You, *J. Phys. Chem. B*, 2005, **109**, 23550–23557.
33 Y. Li, L. Tang and J. Li, *Electrochem. Commun.*, 2009, **11**, 846–849.
34 Z. Wen, Q. Wang and J. Li, *Adv. Funct. Mater.*, 2008, **18**, 959–964.
35 X. Yu and S. Ye, *J. Power Sources*, 2007, **172**, 133–144.
36 J. J. Escard, C. Leclerc and J. P. Contour, *J. Catal.*, 1973, **29**, 31–39.
37 F. Coloma, A. Sepulveda, J. Fierro and F. Rodriguez-Reinoso, *Appl. Catal., A*, 1996, **148**, 63–80.